



	Experiment title: Element-Resolved Ferromagnetic Resonance Detected by XMCD	Experiment number: HE 1867
Beamline: ID08	Date of experiment: from: 13/04/2005 to: 19/04/2005	Date of report: 12/08/2005
Shifts: 18	Local contact(s): Dr. P. Bencok	<i>Received at ESRF:</i>
Names and affiliations of applicants: P. Gambardella and G. Boero <i>Ecole Polytechnique Fédérale de Lausanne, CH-1015 Lausanne</i>		

Experiment HE1867 aimed at developing a novel technique for the analysis of heterogeneous magnetic systems, namely the detection of elemental ferromagnetic resonance (FMR) spectra by means of XMCD on samples resonantly excited at microwave frequencies. The successful outcome of the experiment is reported below.

Our method exploits the XMCD dependence on the relative orientation between the sample magnetization \mathbf{M} and photon polarization \mathbf{P} to detect time-averaged variations of the x-ray absorption signal due to the resonant excitation of precession modes that affect the projection of \mathbf{M} onto its equilibrium direction. The latter is set parallel to \mathbf{P} by an external field \mathbf{B}_0 , as shown in Fig. 1. The experimental setup schematically represented in the figure was mounted and tested prior to the beamtime at the EPF Lausanne by means of conventional FMR methods. It consists of a coplanar waveguide $\lambda/2$ -resonator placed in a static magnetic field \mathbf{B}_0 that can be swept between 0 and ± 0.5 T. A YIG ($\text{Y}_3\text{Fe}_5\text{O}_{12}$) polycrystalline slab was chosen as test sample, owing to its intense FMR response. The sample was positioned at the center of the resonator, which produced a microwave magnetic field $\mathbf{B}_1 \approx 0.1$ mT parallel to the sample surface at its resonance frequency $\omega = 2\pi \times 2.47$ GHz. The experiment was carried out at beamline ID08 using the photon beam generated by its two helical undulators with nearly 100 % circular polarization rate. The beam incidence direction was aligned with \mathbf{B}_0 and set perpendicular to the sample surface. X-ray absorption spectra (XAS) were measured by recording the sample fluorescence yield by means of a Si photodiode as a function of the incident photon energy. X-ray FMR spectra (XFMR) were recorded at fixed photon energy as a function of \mathbf{B}_0 in the presence of the microwave field. For the XFMR measurements, the microwave generator output [Fig. 1(b)] was pulse-modulated at a frequency of 3.5 kHz. The amplified photodiode signal was fed into a lock-in amplifier, which was set to measure the amplitude of the input signal at the pulse-modulation frequency.

The $L_{2,3}$ XMCD spectrum of Fe in YIG is shown in Fig. 2 (a) as $I_{\text{DC}}(\mathbf{P}^+) - I_{\text{DC}}(\mathbf{P}^-)$, where I_{DC} indicates the DC photodiode current measured in standard fluorescence experiments. The largest dichroic effects at the L_3 and L_2 edges are observed at 709.4 and 722.8 eV, respectively. Figures 2 (b) and (c) show the I_{DC} recorded at these energies as a function of \mathbf{B}_0 in the four $\mathbf{P}^+ \mathbf{B}_0^+$ and $\mathbf{P}^- \mathbf{B}_0^+$ configurations. Note that the I_{DC} difference between these configurations, i.e., the XMCD, decreases to zero as \mathbf{B}_0 tends to zero, owing to the negligible remanent magnetization of our sample, while it tends to a constant value for $\mathbf{B}_0 > 0.2$ T owing to the saturation of the magnetization. The XFMR measurements were performed by setting the photon energy to either 709.4 or 722.8 eV and recording the amplitude of the AC photodiode current I_{AC} at the pulse-modulation frequency of \mathbf{B}_1 as a function of \mathbf{B}_0 . Figure 3 shows the XFMR spectra obtained for the different

combinations of \mathbf{P} and \mathbf{B}_0 . In all cases, we observe a peak at $|\mathbf{B}_0| = 0.25$ T, in good agreement with the resonant field $\omega/\gamma + \mu_0 M_s = 0.27$ T given by Kittel's formula for the uniform precession of the magnetization in a perpendicularly magnetized thin plate. Here, $\mu_0 M_s = 0.18$ T for YIG, where M_s is the saturation magnetization. The asymmetric character of the resonance peak and its width ($\Delta B_0 \approx 10$ mT at -3 dB) are attributed to imperfections of the sample surface and edges, and to variations of the demagnetizing field across the sample surface. The key feature of the spectra in Fig. 3 is the reversed sign of the XFMR peak for the $\mathbf{P}^+ \mathbf{B}_0^-$ configurations with respect to $\mathbf{P}^+ \mathbf{B}_0^+$. This, together with the sign inversion at the L_3 and L_2 edge, represents compelling evidence of the XMCD origin and photon energy dependence of the observed signal. By comparing the amplitude of the XFMR peak (15 pA) with the variation of I_{DC} in Figs. 2 (b) and (c) corresponding to the complete reversal of \mathbf{M} (5 nA), the variation of the z-component of the magnetization with respect to its static equilibrium value M_s is estimated to be about 1 %. An interesting point to be investigated further is that the negative and positive XFMR peaks do not have the same amplitude. Part of this effect is due to the asymmetry of I_{DC} at $|\mathbf{B}_0| = 0.25$ T with respect to the intensity level of the demagnetized state of the sample, but additional effects related to the influence of microwave absorption on the fluorescence yield might come into play. The signal amplitude was found to increase linearly with applied microwave power ($\propto B_1^2$), as expected for $B_1 \ll \Delta B_0$. Moreover, we found that I_{DC} and I_{AC} increase linearly with the beam intensity whereas the noise level is proportional to $\sqrt{I_{DC}}$. Therefore, the signal-to-noise ratio can be ameliorated also by maximizing the beam intensity and the solid angle covered by the photodiode.

In conclusion, we have demonstrated a new method to measure continuous-wave FMR spectra based on the core-level absorption of circularly polarized x-rays. The x-ray FMR signal was shown to be energy-dependent, which makes the technique element-sensitive and opens up new possibilities to perform element-resolved FMR in magnetic alloys and multilayers [3]. Given the XAS surface sensitivity, XFMR can be applied to samples with thickness down to a few tens of nm without considerable loss of signal. This makes it straightforward to extend XFMR to metallic samples where the skin-effect limits the penetration of microwave radiation. Future experiments will test the possibility to perform XFMR on metal multilayers and to use the photoelectron yield rather than fluorescence yield detection to further augment the surface sensitivity of the technique. X-ray detection of electron paramagnetic resonance, e.g., on metallorganic compounds, constitutes a possible extension of this technique.

[1] M. Bonfim et al., Phys. Rev. Lett. **86**, 3646 (2001).

[2] W. E. Bailey, L. Cheng, D. J. Keavney, C.-C. Kao, E. Vescovo, and D. A. Arena, Phys. Rev. B **70**, 172403 (2004).

[3] G. Boero, S. Rusponi, P. Bencok, H. Brune, R.S. Popovic, and P. Gambardella, *Appl. Phys. Lett.* (in press).

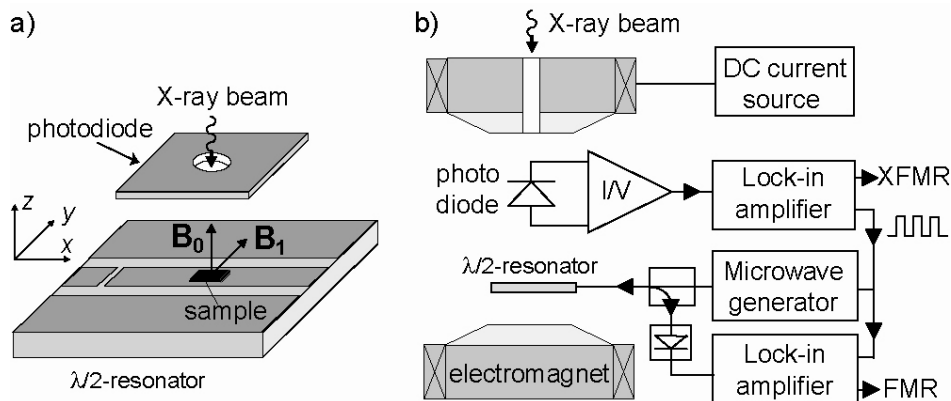


Fig. 1. Schematic representation of the XFMR setup. (a) Resonator, sample, and photodiode (not to scale). (b) Block diagram of the electronics.

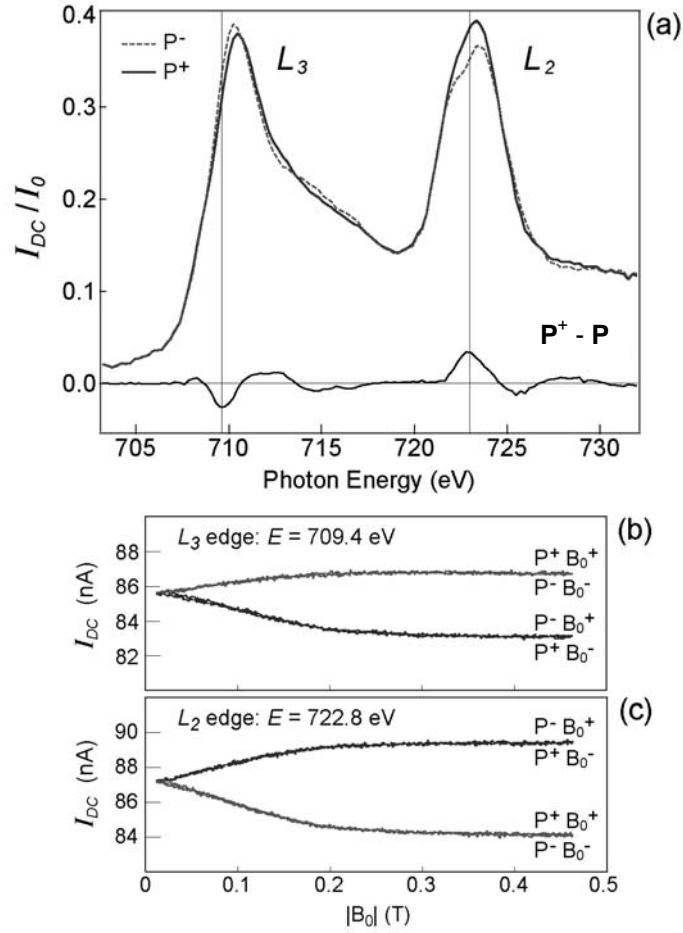


Fig. 2. (a) XAS spectra over L_3 and L_2 edges of Fe recorded with photon polarization parallel (\mathbf{P}^- , dashed line) and antiparallel (\mathbf{P}^+ , solid line) to $\mathbf{B}_0 = -0.5$ T. The DC fluorescence current I_{DC} is shown normalized to the incident photon flux I_0 , measured by the drain current of the first refocussing mirror upstream of the sample. The XMCD spectrum is shown at the bottom. The spectra are not corrected for self-absorption effects. (b) I_{DC} vs. \mathbf{B}_0 recorded at the L_3 edge ($E=709.4$ eV) and (c) and L_2 ($E=722.8$ eV).

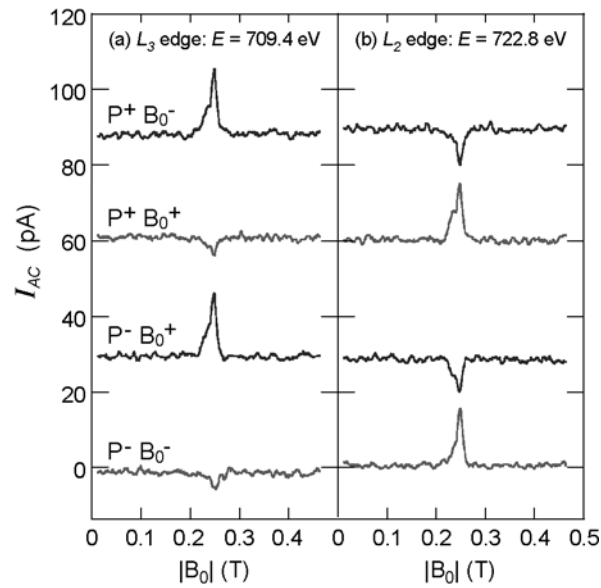


Fig. 3. XFMR spectra of Fe in YIG: AC component of the photodiode current at the pulse-modulation frequency of \mathbf{B}_1 as a function of $|\mathbf{B}_0|$ and \mathbf{P} . (a) L_3 edge ($E=709.4$ eV) and (b) L_2 edge ($E=722.8$ eV). The spectra have been offset for clarity.